High energy radiation from Centaurus A

2009 New J. Phys. 11 065017

(http://iopscience.iop.org/1367-2630/11/6/065017)

New Journal of Physics
The open-access journal for physics

High energy radiation from Centaurus A

M Kachelrieß[1,4], **S Ostapchenko**[1,2] **and R Tomàs**[3]

[1] Institutt for fysikk, NTNU, Trondheim, Norway
[2] D V Skobeltsyn Institute of Nuclear Physics, Moscow State University, Moscow, Russia
[3] II Institut für Theoretische Physik, Universität Hamburg, Hamburg, Germany
E-mail: Michael.Kachelriess@ntnu.no

New Journal of Physics **11** (2009) 065017 (13pp)
Received 17 June 2008
Published 30 June 2009
Online at http://www.njp.org/
doi:10.1088/1367-2630/11/6/065017

Abstract. We calculate, for the nearest active galactic nucleus (AGN), Centaurus A (Cen A), the flux of high-energy cosmic rays (CR) and of accompanying secondary photons and neutrinos expected from hadronic interactions in the source. We use as the two basic models for the generation of ultrahigh-energy cosmic rays (UHECR) shock acceleration in the radio jet and acceleration in the regular electromagnetic field close to the core of the AGN. While scattering on photons dominates in scenarios with acceleration close to the core, scattering on gas becomes more important if acceleration takes place along the jet. Normalizing the UHECR flux from Cen A to the observations of the Auger experiment, the neutrino flux may be marginally observable in a $1\,\mathrm{km}^3$ neutrino telescope, if a steep UHECR flux $\mathrm{d}N/\mathrm{d}E \propto E^{-\alpha}$ with $\alpha = 2.7$ extends down to 10^{17} eV. The associated photon flux is close to or exceeds the observational data of atmospheric Cherenkov and γ-ray telescopes for $\alpha \gtrsim 2$. In particular, we find that already the present data favour either a softer UHECR injection spectrum than $\alpha = 2.7$ for Cen A or a lower UHECR flux than expected from the normalization to the Auger observations.

[4] Author to whom any correspondence should be addressed.

Contents

1. Introduction **2**
2. Source and acceleration models for Cen A **3**
2.1. Source parameters, the primary photon field and the gas column density 3
2.2. CR acceleration, propagation and interactions in the source 5
3. CR, photon and neutrino fluxes **8**
4. Conclusions **10**
Acknowledgments **11**
References **11**

1. Introduction

Progress in cosmic ray (CR) physics has been hampered for a long time by the deflection of charged CRs in magnetic fields, preventing the identification of individual sources. Numerous searches for anisotropies and correlation studies have been performed, without reaching unanimous conclusions [1]. Using neutral messengers that should be produced as secondaries in proton–photon and proton–proton interactions close to the source for the identification of the sources has its own problems: first, secondary photons generated by hadronic CR interactions are difficult to disentangle from photons produced by synchrotron radiation or inverse Compton scattering of electrons. Moreover, high-energy photons are strongly absorbed both in the source and propagating over extragalactic distances. By contrast, the extremely large mean free path of neutrinos together with the relatively poor angular resolution of neutrino telescopes ($\sim 1^\circ$) and the small expected event numbers makes the identification of extragalactic sources challenging when using only the neutrino signal. Performing neutrino astronomy beyond the establishment of a diffuse neutrino background, therefore, most likely requires additional input, either timing or angular information from high-energy photon or CR experiments.

The recently published evidence [2] for a correlation of the arrival directions of ultrahigh-energy (UHE) CRs (UHECRs) observed by the Pierre Auger Observatory (PAO) with active galactic nuclei (AGN) may provide a first test case for successful 'multi-messenger astronomy'. In particular, Abraham *et al* [2] find two events within the search bin of 3.1° around the nearest active galaxy, Centaurus A (Cen A or NGC 5128), which is located close to the supergalactic plane. At present, this correlation has only $3\,\sigma$ C.L., and other source types that follow the large-scale structure of matter would also result in an excess of events along the supergalactic plane. Independent evidence for the AGN source hypothesis is the characteristic bias of AGN with respect to the large-scale structure that is indeed reflected in the angular distribution of the observed UHECR arrival directions [3]. On the other hand, the correlation with AGN is not confirmed by the data from the HiRes experiment [4]. It is therefore timely to study the potential of high-energy neutrino and photon observations for scrutinizing the correlation signal suggested by the Auger collaboration.

The idea that neutrinos and photons are produced as secondaries in CR interactions close to the core of AGN has a long history [5]. In particular, the diffuse neutrino and photon fluxes from all AGN have been studied in great detail [6]–[8]. Moreover, the expected neutrino and photon fluxes from Cen A were discussed recently in view of the PAO results in [9, 10] and [11], respectively. The present work extends these later studies by calculating both neutrino and

photon secondary fluxes and by modelling the source and particle interactions in more detail. Acceleration of protons to energies as high as 10^{20} eV in Cen A is used as an assumption that we discuss only as far as the source parameters are concerned.

2. Source and acceleration models for Cen A

2.1. Source parameters, the primary photon field and the gas column density

2.1.1. Accretion. A general review of the properties of Cen A, which is classified as FR I radio galaxy and as Seyfert 2 in the optical, is given in [12][5]. Its observed spectral energy distribution (SED) of electromagnetic radiation is discussed in detail by Steinle [13]. Although Cen A is the nearest active galaxy with its distance[6] of $D = 3.8$ Mpc [14], there are a number of difficulties in deducing the photon distribution $n_\gamma(\mathbf{x}, \mathbf{p})$ that serves as the target for hadronic interactions from observational data. Firstly, the resolution of e.g. x-ray satellites such as Chandra (0.5″) or XMM-Newton (5″) is not sufficient to resolve the core of the AGN. Secondly, part of the emitted radiation is heavily absorbed by the dust lane hiding the AGN core. Thirdly, it is useful to distinguish between primary photons that serve as targets for hadronic interactions and secondary photons produced therein. Finally, the observed photon flux is at most energies probably dominated by photons produced in purely electromagnetic processes.

We prefer therefore to model the primary photon field around the AGN core guided by the simplest possible theoretical model [15]. The thermal emission from a geometrically thin, optically thick Keplerian accretion disc is described by the temperature profile

$$T(r) = \left(\frac{3GM\dot{M}}{8\sigma\pi r^3}\left[1 - (R_0/r)^{1/2}\right]\right)^{1/4}. \tag{1}$$

Within this simple model, the mass M of the central supermassive black hole (SMBH), its accretion rate $\dot{M}$ and the inner edge of the accretion disc R_0 fix the main part of the primary electromagnetic radiation. Recent estimates for M vary in the range $(0.5\text{–}2) \times 10^8 M_\odot$ [16]. We will use $M = 1 \times 10^8 M_\odot$ and thus the Schwarzschild radius is $R_s = 3 \times 10^{13}$ cm. The angular momentum of the SMBH in Cen A is not known, so we use as the smallest radius of the acceleration and of the emission region the radius of the last stable orbit for a Schwarzschild black hole, $R_0 = 3R_s \approx 1 \times 10^{14}$ cm.

The accretion rate $\dot{M}$ and accretion efficiency $\eta = L/(\dot{M}c^2)$ were fitted in [17] to Chandra and XMM-Newton observations assuming spherical (Bondi) accretion. The obtained accretion rate $\dot{M} = 6 \times 10^{-4} M_\odot\,\mathrm{yr}^{-1}$ should be considered as a lower limit, because it does not account for the accretion of gas too cool to emit x-rays[7]. In particular, it has been argued in [19, 20] that the heavy x-ray absorption and the high metallicity indicate accretion of cold gas.

Integrating the surface brightness $D = \sigma T^4$ over the finite accretion disc for the chosen values of M, $\dot{M}$ and R_0 reproduces the characteristic blue bump [21]. Because of the relatively small accretion rate, the bump is shifted towards somewhat lower frequencies compared with the standard case. The dust lane of Cen A prevents such a bump being seen by us directly in the SED of Cen A, but the observed HII line emission that is best explained by UV irradiation from the central nucleus is indirect evidence for its existence [22].

[5] See also http://www.mpe.mpg.de/Cen-A/ for an extensive list of references for Cen A.
[6] At this distance $1'' = 18$ pc.
[7] The numerical value for $M_{\mathrm{Bondi}}c^2$ and thus also for η in [17] contains a numerical error [18].

Table 1. The luminosities, efficiencies and normalization constants in different wavelength ranges.

Band	L_i (erg s^{-1})	η	$\tilde{\eta}$	K_i (cm^{-3} eV^{-1})
γ-ray	5.0×10^{42}	15%	3.3×10^{-4}	–
X-ray	4.8×10^{41}	1.5%	3.3×10^{-5}	8×10^{11}
UV	3.6×10^{42}	10%	2.4×10^{-4}	1×10^{13}

Since the surface brightness drops fast with the radius, $D \propto r^{-3}$, most of the radiation is emitted close to the core, (3–15)R_s, cf also [23]. To simplify our simulation, we consider therefore the following one-dimensional model for the source. We describe the accretion disc as a sphere of radius $R_1 = 15R_s$ filled with a homogeneous, isotropic photon field radiating photons with the same spectrum $n_\gamma(\varepsilon)$ from each point on a 'photosphere' with radius R_1.[8] We model the energy dependence of n_γ by

$$n_\gamma(\varepsilon) = K_{\rm UV} \begin{cases} 25\,\varepsilon_{\rm eV}, & \varepsilon_{\rm eV} < 0.2, \\ \varepsilon_{\rm eV}^{-1}, & 0.2 < \varepsilon_{\rm eV} < 5, \\ 0.1\,\varepsilon_{\rm eV}^{2} \exp(-\varepsilon_{\rm eV}/2), & \varepsilon_{\rm eV} > 5, \end{cases} \tag{2}$$

with $\varepsilon_{\rm eV} \equiv \varepsilon/{\rm eV}$. The exponential cut-off is connected with the maximal temperature of the disc close to R_0. Finally, we assume that a hot corona produces an additional x-ray component,

$$n_{\rm X}(\varepsilon) = K_{\rm X} \varepsilon_{\rm eV}^{-1.7}\,, \tag{3}$$

where the exponent -1.7 is chosen to agree with the x-ray observations from Evans *et al* [17] and Markowitz *et al* [20] and we use as high-energy cut-off $\varepsilon = 100\,{\rm keV}$.

2.1.2. Normalization. The accretion rate $\dot{M} = 6 \times 10^{-4} M_\odot\,{\rm yr}^{-1}$ determines together with the accretion efficiencies η_i the luminosity L_i in the wavelength range i, $L_i = \eta_i \dot{M} c^2$. For the x-ray range, we use $L_{\rm X} = 4.8 \times 10^{41}\,{\rm erg\,s}^{-1}$ in the 2–10 keV range according to the observations [17, 20] together with

$$L_i = \pi R_1^2\, c \int {\rm d}\varepsilon\, \varepsilon n_\gamma(\varepsilon) = \eta_i L_{\rm Bondi} = \eta_i \dot{M} c^2\,, \tag{4}$$

giving $K_{\rm X} = 8 \times 10^{11}\,{\rm cm}^{-3}\,{\rm eV}^{-1}$ and $\eta_{\rm X} = 1.5\%$. The γ-ray luminosity $L_\gamma = 5 \times 10^{42}\,{\rm erg\,s}^{-1}$ observed by COMPTEL and OSSE [25] corresponds to $\eta_\gamma = 15\%$. Finally, we choose the normalization of the UV bump, $K_{\rm UV}$ in equation (2), as $\eta_{\rm UV} = 10\%$.

The used numerical values of the various normalization constants are summarized in table 1. In this table, we report also the resulting efficiencies $\tilde{\eta} = L_i/L_{\rm Edd}$ relative to the Eddington luminosity, $L_{\rm Edd} = 1.5 \times 10^{46}\,{\rm erg\,s}^{-1}$, of a $10^8 M_\odot$ black hole. The combined value of $\sum_i \tilde{\eta}_i$ is in the range of advection-dominated accretion and thus the formation of a geometrically thin, optically thick accretion disc for Cen A is not guaranteed. We will nevertheless assume the

[8] In addition to being a technical simplification, it was suggested that a sphere of radius (0.1–1) pc filled with a nearly isotropic photon field could be realized by the scattering of UV photons from the accretion disc on clouds in the BLR region, cf [24].

existence of such a standard Shakura–Sunyaev accretion disc, keeping in mind however that the derived values for the photon density should be considered as upper limits.

For large distances, $r \gg R_1$, the photon field emitted from the photosphere of radius R_1 scales as $n_\gamma(r) \propto (R_1/r)^2$ and has approximately a distribution of momentum vectors with $\cos\vartheta = \mathbf{p}\cdot\mathbf{r}/(|\mathbf{p}|\,|\mathbf{r}|) \geqslant 1-(R_1/r)^2$. Thus, we have to distinguish two cases: either photons and/or CRs are distributed isotropically or both are non-isotropic. The latter case is realized when charged particles propagate along the (regular) field lines and primary photons stream nearly radially outwards for $r \gg R_1$. Above the threshold $E \sim 10^{16}$ eV, the resulting interaction depth is $\tau_{p\gamma} \sim 3$.

The PAO data used in the analysis [2] correspond to an exposure $\Xi = 9000\,\mathrm{km^2\,yr\,sr}$ with maximal zenith angle $\vartheta_{\max} = 60^\circ$. The correlation signal with AGN was maximized for the threshold energy $E_{\rm th} = 6\times10^{19}$ eV and the angular bin size 3.1°. For these values, two events were found in the angular bin around Cen A. Cen A is close enough to the Earth that energy losses of CRs with energy close to $E_{\rm th}$ can be neglected, cf figure 1 of [26]. Assuming that both events indeed originate from this AGN, the integral CR flux above $E_{\rm th}$ on the Earth from Cen A is

$$F(>E_{\rm th}) = \frac{2\,\Omega}{R\,\Xi} = 2\times10^{-3}\,\mathrm{km^{-2}\,yr^{-1}}. \tag{5}$$

Here, $\Omega \approx 9$ sr is the field-of-view of the PAO and $R = \eta(\delta_{\rm s})/\langle\eta(\delta)\rangle \approx 0.95$ is the ratio of the exposure $\eta(\delta_{\rm s})$ at the declination $\delta_{\rm s} = -43.0^\circ$ of Cen A and the average exposure $\langle\eta\rangle$.

2.1.3. Gas column density and proton–proton interactions. Markowitz *et al* [20] fitted Suzaku observations of Cen A with several absorption models. The primary x-ray component was found to be absorbed by the column density $X = 1\times10^{23}\,\mathrm{cm^{-2}}$, while a less bright component is more heavily absorbed with $X = 7\times10^{23}\,\mathrm{cm^{-2}}$. These results can be interpreted either as an indication of a clumpy structure of the gas or of two different x-ray sources, e.g. from accretion and from jet emission. The resolution of these observations, however, is rather limited, and the value of the column density is therefore biased by the dense torus. A more representative determination of the mean density of the gas around the core of Cen A was possible with XMM-Newton and Chandra observations. Kraft *et al* [27] determined the density of the interstellar medium around the core of Cen A as $n_{\rm H} = n_0[1+(r/r_0)^2]^{-0.6}$ with $n_0 = 0.04\,\mathrm{cm^{-3}}$ and $r_0 = 0.5$ kpc. Finally, Worrall *et al* [28] found an average hydrogen density $X = 1.5\times10^{21}\,\mathrm{cm^{-2}}$ along the radio jet starting from a projected distance of 0.3 kpc up to 2.5 kpc. With $d = 0.4$ kpc as the diameter of the jet and assuming that the jet axis is almost perpendicular to the line-of-sight [29], an average density $n_{\rm H} \approx X_{\rm H}/d \approx 1.7\,\mathrm{cm^{-3}}$ follows.

2.2. CR acceleration, propagation and interactions in the source

X-ray observations of Cen A allow one to trace the acceleration sites of electrons along the radio jet, because their synchrotron loss length is short compared with the extension of the jet. The strong dependence of synchrotron emission on the mass of the radiating particle implies that the SED is, apart from the highest energies, dominated by electromagnetic interactions of electrons and that therefore the acceleration site and mechanism for electrons and protons may differ. Although various proposals for the acceleration of protons to UHE exist, we restrict ourselves to two basic models, namely shock acceleration in the radio jet and acceleration in the regular electromagnetic field close to the core of the AGN. These two models are characterized

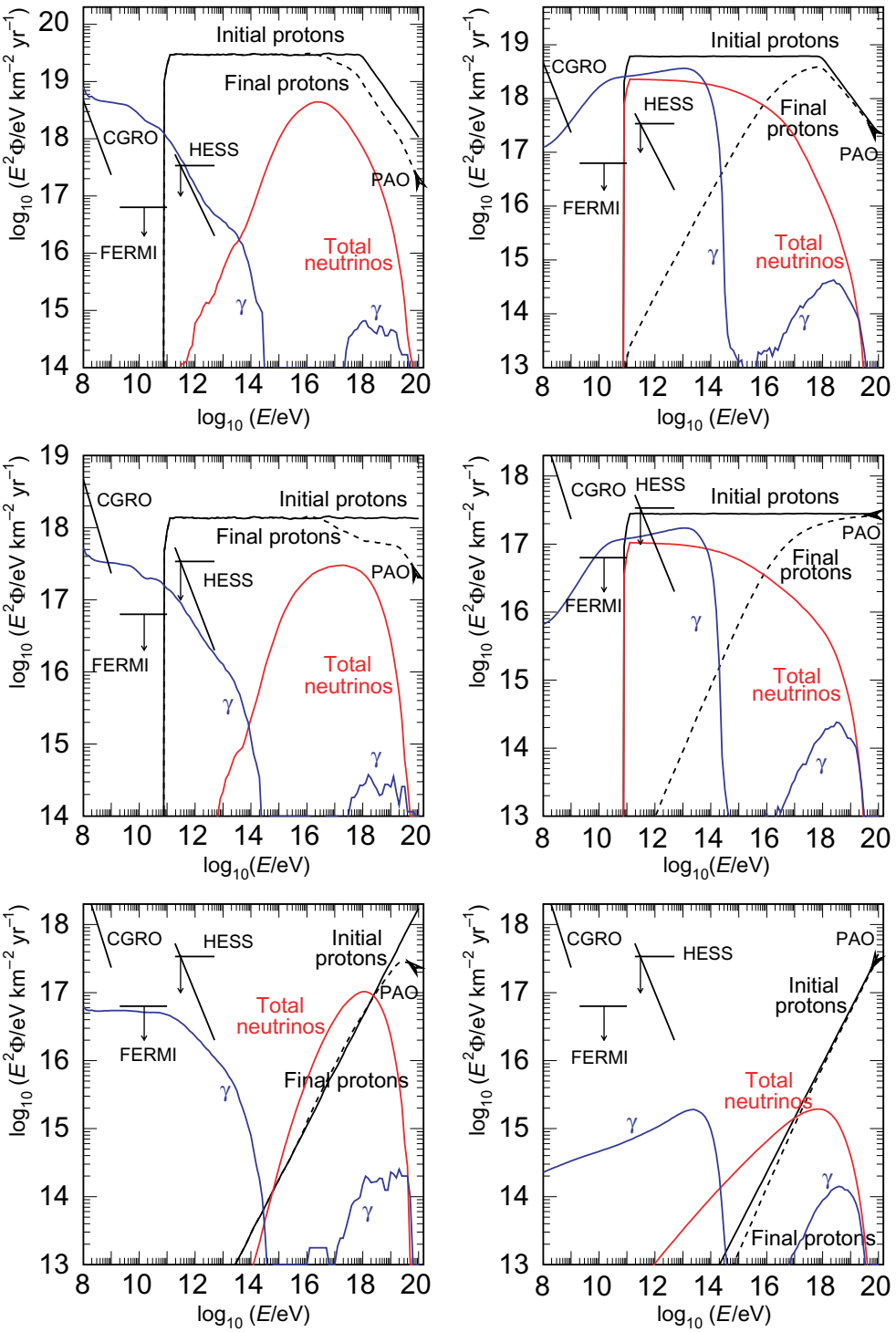

Figure 1. Particle fluxes $F(E)$ from Cen A normalized to the PAO data as a function of the energy E. Top panels: broken power-law with $\alpha = 2$ and 2.7 and break energy $E_b = 10^{18}$ eV; middle panels: $\alpha = 2$; bottom panels: $\alpha = 1.2$; left panels: acceleration close to the core; right panels: in the jet; the initial protons (solid black line), final protons (dashed black line), photons (blue line), and sum of all neutrinos (red line).

by a rather different set of parameters and the secondary fluxes in several other models may be obtained by 'appropriate interpolation'. We neglect relativistic effects, because of the moderate Lorentz factors observed in Cen A and the large angle between the jet axis and the line-of-sight.

2.2.1. Acceleration in regular fields near the core. Acceleration close to the core could proceed either via shock acceleration in accretion shocks [30] or via acceleration in regular fields. The former case is disfavoured since the acceleration rate is smaller than the rate of photon–pion energy losses [31]. Therefore, we consider here only acceleration in regular fields close to the core. Among the possibilities discussed in the literature are electromagnetic winds from the BH/disc magnetosphere [32, 33], and unipolar induction around a Kerr BH [34, 35]. The regular magnetic field close to the core consists of a toroidal component in the accretion disc and a poloidal field component $B_{\rm p} = B_0(R_0/r)^{\beta}$. For field strengths $B_0 \sim 1$ kG, acceleration to energies around 10^{20} eV is possible. Since the curvature radius $R_{\rm C}$ of the field lines is typically large, curvature radiation of protons is not very effective. Moreover, protons move mainly parallel to the field lines and thus also synchrotron losses are suppressed. Because of our simplified one-dimensional geometry, we assume that the combined effect of synchrotron and curvature radiation is such that it does not affect protons but acts as main energy loss for electrons. The other remaining free parameter in this model, the injection point of the CRs, is fixed at $r = 6R_{\rm s}$.

The required magnetic field strength for acceleration to 10^{20} eV is an order of magnitude higher than one would expect from equipartition, $B^2/8\pi \sim L/4\pi R_0^2 c$. The currently low accretion rate and small luminosity of Cen A disfavour therefore, acceleration close to the core as the acceleration mechanism, if Cen A was not in the past in a state of higher activity.

2.2.2. Acceleration in the radio jet. Rachen and Biermann [36] suggested the hot spots in FR II radio galaxies as sites of UHECR acceleration. These spots are formed as termination shock of the supersonic jets in the intergalactic medium and are especially prominent in FR II jets. They are instead dim or absent in weak FR I sources, most likely because strong turbulent dissipation in the propagation phase reduces the momentum finally released at the termination shock. Nevertheless, e.g. Romero *et al* [37] argued that, at the 'hot spot' in Cen A, acceleration of protons to UHE occurs. The projected size of the hot spot is $R_{\rm HS} \approx 1.7$ kpc, containing magnetic fields with strengths $B \approx 0.5$ mG. Alternatively, protons could be accelerated along the whole extension of the radio jet, extending a projected distance of 6 kpc from the nucleus. In this case, protons have to diffuse through the x-ray photons emitted by accelerated electrons and, more importantly, through the hydrogen gas observed in the jet.

Thus, we shall use acceleration in the jet as our second basic scenario. More precisely, we consider as acceleration region for protons a cylinder of length $l = 4$ kpc and diameter $d = 0.3$ kpc, similar to the emission volume of x-rays observed by Chandra. Diffusion in the turbulent magnetic fields will increase the interaction depth. We choose as the field strength $B = 0.2$ mG, we set the coherence length as conservatively equal to the length $l_{\rm c} = 1$ kpc and we use $a = \frac{1}{2}$ for the energy dependence of the diffusion coefficient, $D(E) \propto E^a$, corresponding to a Kraichnan fluctuation spectrum. The choice $a = \frac{1}{2}$ is intermediate between the often assumed Bohm and Kolmogoroff diffusions and is close to the numerical results of Casse *et al* [38].

2.2.3. Relative importance of photon and proton targets. In the case of acceleration close to the core, either in accretion shocks or regular electromagnetic fields, UV photons are the most important scattering targets and the interaction depth for photo–hadron interactions can reach $\tau_{p\gamma} \sim$ few. In all other cases, $\tau_{p\gamma}$ will be reduced at least by a factor $\sim 10 R_s/l$, where l is the typical dimension of the acceleration region. Diffusion increases the effective size of the source, but this effect becomes noticeable mainly at energies below the threshold for photon–hadron interactions. As a rule of thumb, photo–hadron interactions are, therefore, only important when the acceleration takes place close to the core.

The importance of proton–proton interactions depends more strongly on the concrete model assumptions—as the scatter in the observed column density X of gas shows. Moreover, the accretion rate may be time-dependent and matter close to the core is concentrated in clumps. Thus both the CR luminosity L_{CR} and the interaction depth τ_{pp} can vary significantly depending on the model assumptions. While the importance of gas as the target close to the core is uncertain, the Chandra observations indicate that p–p scattering is the main source of CR interactions in the jet.

2.2.4. Energy spectrum and interactions. We consider three cases for the generation spectrum $dN/dE \propto E^{-\alpha}$ of UHECRs: (i) A power law with $\alpha \approx 2$ as conventionally predicted from first-order Fermi acceleration with non-relativistic shocks. (ii) A broken power law with break energies $E_b = 10^{17}$ eV and $E_b = 10^{18}$ eV, respectively, and $\alpha = 2.7$ for $E > E_b$ as suggested by the dip interpretation of the experimental data [39]. Since the steepening of the observed diffuse spectrum may result from a distribution of maximal energies dn/dE_{max} [40], the present UHECR observations do not distinguish between these two possibilities, even if one assumes that extragalactic sources dominated the flux down to 10^{17} eV. Note also that $\alpha = 2.7$ is consistent with the observed radio spectrum of most AGN. In order to weaken the energy demands of Cen A, we extend the $\alpha = 2.7$ spectrum with $\alpha = 2$ below E_b. (iii) A flat spectrum with $\alpha = 1.2$ and most energy concentrated at E_{max}, as expected for a 'linear accelerator'. In all three cases we use $E_{max} = 10^{20}$ eV.

Hadronic interactions are simulated with an extension of the Monte Carlo code described in [41][9], including the possibility of a non-thermal and anisotropic photon field $n_\gamma(\mathbf{x}, \mathbf{p})$ and of proton–proton interactions. Electromagnetic processes[10] such as pair production and inverse Compton scattering of electrons and photons both inside the source and on IR, cosmic microwave background (CMB) and radio photons are also taken into account. Finally, diffusion is simulated as described in [41].

3. CR, photon and neutrino fluxes

The left and right panels of figure 1 display the particle fluxes $F(E)$ predicted from Cen A as a function of the energy E in the case of acceleration close to the core and in the jet, respectively. In addition to the injected proton flux (black solid line), we show the flux of protons (black dashed) arriving on the Earth. The final proton flux is reduced by interactions by a factor of ≈ 2 above the threshold energy $\sim 10^{16}$ eV for photon–proton interactions (left), while diffusion in

[9] The Monte Carlo code makes use of the publicly available programs JETSET (Sjostrand [42]), SIBYLL (Fletcher *et al* [42]), SOPHIA (Mücke *et al* [42]) and QGSJETII (Ostapchenko [42]).

[10] A description of our treatment of electromagnetic cascades and results will be presented elsewhere.

the jet increases the interaction depth for lower energies (right panels), resulting in the effective production of secondaries.

The photon flux at the Earth after cascading in the source and on the extragalactic background light (EBL) consists of two contributions: (i) photons produced in the source, which survive their subsequent travel to the observer without interactions with the EBL; and (ii) photons produced during the cascade on the EBL. While the former are always observed as a point-like contribution from a point-like source, the latter are characterized by a finite angular spread, due to the deflections of cascade electrons in the extragalactic magnetic field (EGMF). Depending on the strength of the latter and on the experimental resolution, the second contribution may be observed as a halo around the source [43] while contributing only partially to the unresolved point-like flux. Because of the proximity of Cen A, deflections in the EGMF have a—compared with the overall uncertainties—negligible influence on the calculated photon spectra.

The photon flux at the Earth after cascading in the source and on the ELB is shown as a solid blue line together with the combined fit to EGRET, OSSE and COMPTEL observations of Cen A from Steinle *et al* [25], the HESS limit from Aharonian *et al* [44] for $\alpha = 2$ and $\alpha = 3$, and the FERMI sensitivity [45] for a 5σ detection of a point source in 1 year. The predicted spectrum shows the typical suppression above the pair production threshold on the CMB at $E \approx 200\,\mathrm{TeV}$. Since the CR spectra are normalized to the integral UHECR flux above $E_{\mathrm{th}} = 5.6 \times 10^{19}\,\mathrm{eV}$, steeper spectra result in larger secondary fluxes at low energies. In particular, the photon flux overshoots the HESS limit or the Compton Ganima Ray Observatory (CGRO) observations in the case of a broken power-law injection spectrum. Thus, already the present observational data favour either softer UHECR spectra than $\mathrm{d}N/\mathrm{d}E \propto E^{-2.7}$ for Cen A or a lower UHECR flux than expected from the normalization to the Auger observations. Note however that our normalization relies on only two events and has therefore a large statistical uncertainty. On the other hand, the determination of the energy scale of UHECR experiments is notoriously difficult and it has been argued that the PAO energy scale should be shifted up to obtain agreement with the spectral shape predicted by e^+e^- pair production [39].

Comparing the neutrino flux at $10^{16}\,\mathrm{eV}$ for the different models allows one to judge how strongly the predicted neutrino event number depends on the slope of the CR spectrum. Going from a broken power law with $\alpha = 2.7$ at UHE to $\alpha = 1.2$ reduces between three and four orders of magnitude the neutrino flux at 100 TeV. Calculating the expected event number in a neutrino telescope requires a definite choice of the experiment. Cen A is, from the location of Icecube, only visible from above, and thus the background of atmospheric muons allows only the use of contained events that carry essentially no directional information ($\delta\vartheta \sim 30^\circ$). For the calculation of the number of contained events expected in Icecube, we use as effective volume $V = 1\,\mathrm{km}^3$, as threshold $E_{\mathrm{min}} = 100\,\mathrm{TeV}$ and assume 100% efficiency above E_{min} and we use the CTEQ5 neutrino–nucleon cross sections [46]. By contrast, a neutrino telescope in the Mediterranean could make use of the muon signal and the directional information. In this case, the rate R of muon events can be approximated by

$$R = A \int_{E_{\mathrm{min}}}^{\infty} \mathrm{d}E\, S(E) F_{\nu_\mu}(E) P(E, E_{\mathrm{min}}) \tag{6}$$

with $A = 1\,\mathrm{km}^2$, the probability $P(E, E_{\mathrm{min}}) = N_A \langle R(E, E_{\mathrm{min}}) \rangle \sigma_{\nu N}$ that a muon reaches with $E > E_{\mathrm{min}}$ the detector and the angular averaged shadowing factor $S(E_\nu)$ accounting for attenuation of the neutrino flux in the Earth [47]. The resulting event numbers both for cascade

Table 2. The injected CR luminosity $L_{\rm CR}$ and the number of neutrino events expected per year observation time for different energy slopes and acceleration scenarios.

	Jet				Core			
α or $E_{\rm b}$ (eV)	1.2	2.0	10^{18}	10^{17}	1.2	2.0	10^{18}	10^{17}
L_{CR} (10^{40} erg s^{-1})	0.35	0.97	5.2	5.2	1.1	2.2	11	10
Contained no. of ν yr^{-1}	8×10^{-5}	0.02	0.4	2.0	7×10^{-4}	0.01	0.3	0.9
No. of μ yr^{-1}	4×10^{-5}	7×10^{-3}	0.2	0.7	3×10^{-4}	7×10^{-3}	0.1	0.5

and shower event number per year observation time are summarized in table 2 together with the input CR luminosity. Note that the cut-off in the neutrino spectra below 100 GeV that is visible in the upper right panels of figure 1 is artificial, since we neglect neutrinos with lower energies in our simulation.

In summary, we predict that for all cases where there is a marginal chance to detect a neutrino signal from Cen A, atmospheric Cherenkov telescopes and/or γ-ray satellites such as FERMI should detect previously a photon signal from Cen A. The main reason for this result—that is in contradiction to earlier expectations, cf [48]—is the cascading of photons in the anisotropic photon field close to the source.

Finally, we remark that we assumed for the calculation of all fluxes isotropic emission. This is well justified in the case of stochastic acceleration in the jet, because of the small gamma factors of the observed matter flows in the jet and the large angle between the jet and the line-of-sight. In the case of acceleration close to the core, protons move along the field lines and thus the emission is rather anisotropic. Since we used the UHECR flux towards our line-of-sight as normalization, the total UHECR luminosity of Cen A is therefore larger than the one estimated in table 1. On the other hand, the predicted number of neutrino events is not affected by the anisotropy, since the ratio of neutrino and UHECR fluxes is roughly independent of the considered direction. By contrast, TeV photons as final products of electromagnetic cascades are more effectively isotropized than UHECRs. This effect will slightly increase the TeV photon flux compared with the isotropic case assumed in figure 1.

The expected neutrino and photon fluxes from Cen A were discussed recently in view of the PAO results in a rather qualitative way in [9]–[11], respectively. Our case of acceleration close to the core and a broken power law corresponds roughly to the set-up of Cuoco and Hannestad [9], but the results differ by the large factor of 30. One possible explanation for this difference is that their neutrino flux drops faster than we found. Halzen and O'Murchadha [10] assumed p–p interactions on gas close to the core with $\tau_{\rm pp} \sim$ few as production mechanism. The obtained event numbers agree well taking into account the differences in the assumptions used. Finally, Gupta [11] discussed photons from hadronic interactions in Cen A. This work did not include the effect of electromagnetic cascading and the conclusions are therefore difficult to compare.

4. Conclusions

We have calculated the flux of high-energy CRs and of accompanying secondary photons and neutrinos expected from Cen A. We modelled the distribution of target photons and gas guided

by the simplest theoretical model for the accretion disc and by observational data, respectively. The production of secondaries and the electromagnetic cascading of electrons and photons were simulated with a Monte Carlo procedure.

In contrast with previous works, we showed that scattering on gas becomes important if acceleration takes place along the jet. Moreover, we found that a source that has an interaction depth $\tau_{p\gamma} \gtrsim 1$ can be observed in the 1–100 TeV range by atmospheric Cherenkov telescopes. In addition to these more technical results, we have shown that a combination of the old CRGO observations and the limits from atmospheric Cherenkov telescopes can be used to constrain currently favoured UHECR models. In particular, we found that these data favour either a softer UHECR injection spectrum than $\mathrm{d}N/\mathrm{d}E \propto E^{-2.7}$ for Cen A or a lower UHECR flux than expected from the normalization to the Auger observations.

One should remember, however, the following main underlying uncertainties in interpreting our results: The normalization of all fluxes is based on the assumption that two UHECR protons in the PAO data originate from Cen A. Note that several authors have argued that a larger number of events originates from Cen A [49]. Apart from the purely Poisson error, the normalization may be influenced by deflections in (extra-) galactic magnetic fields, the uncertainty in the energy scale of PAO, and a possible admixture of heavy nuclei. Deflections of UHECRs result in their delayed arrival with respect to photons and neutrinos, introducing an additional source of uncertainty in their relative normalization. Moreover, our model parameters (M, $\dot{M}$, η_{UV},...) and even such basic parameters as the distance to Cen A have sizeable uncertainties. Last but not least, we have made several simplifying assumptions like the use of a one-dimensional geometry and the omission of the acceleration process: We only *postulated* that acceleration to 10^{20} eV is possible in the environment of Cen A, without demonstrating it for a concrete model. Despite these drawbacks, it is remarkable that γ-ray and TeV observations of Cen A allow one even now to constrain currently favoured UHECR models. The potential of neutrino telescopes to observe Cen A depends strongly on the steepness of the UHECR generation spectrum. A neutrino telescope in the Northern Hemisphere would be very useful for this task.

Acknowledgments

We thank the anonymous referees, Dan Evans and Elisa Resconi for their useful comments and Alessandro Cuoco for discussions that initiated this work. SO and RT acknowledge support from the Deutsche Forschungsgemeinschaft within the Emmy Noether programme and SFB 676, respectively.

References

[1] Berezinsky V S, Bulanov S V, Dogiel V A, Ginzburg V L and Ptuskin V S 1990 *Astrophysics of Cosmic Rays* (Amsterdam: North-Holland)
Nagano M and Watson A A 2000 *Rev. Mod. Phys.* **72** 689
Kachelrieß M 2007 *Nucl. Phys. Proc. Suppl.* **165** 272 (arXiv:astro-ph/0610862)
[2] Abraham J *et al* (PAO Collaboration) 2007 *Science* **318** 939 (arXiv:0711.2256 [astro-ph])
Abraham J *et al* (PAO Collaboration) 2007 arXiv:0712.2843 [astro-ph]
[3] Cuoco A *et al* 2008 *Astrophys. J.* **676** 807 (arXiv:0709.2712 [astro-ph])
[4] Abbasi R U *et al* (HiRes Collaboration) (arXiv:0804.0382 [astro-ph])

[5] Berezinsky V 1977 *Proc. Neutrino (Elbros)*
Eichler D 1979 *Astrophys. J.* **232** 106
[6] Stecker F W, Done C, Salamon M H and Sommers P 1991 *Phys. Rev. Lett.* **66** 2697
Stecker F W, Done C, Salamon M H and Sommers P 1992 *Phys. Rev. Lett.* **69** 2738 (erratum)
Stecker F W 2005 *Phys. Rev.* D **72** 107301 (arXiv:astro-ph/0510537)
Szabo A P and Protheroe R J 1994 *Astropart. Phys.* **2** 375 (arXiv:astro-ph/9405020)
[7] Mannheim K 1995 *Astropart. Phys.* **3** 295
Atoyan A M and Dermer C D 2003 *Astrophys. J.* **586** 79 (arXiv:astro-ph/0209231)
Atoyan A M and Dermer C D 2004 *New Astron. Rev.* **48** 381 (arXiv:astro-ph/0402646)
[8] Semikoz D V and Sigl G 2004 *J. Cosmol. Astropart. Phys.* JCAP04(2004)003 (arXiv:hep-ph/0309328)
[9] Cuoco A and Hannestad S 2007 arXiv:0712.1830 [astro-ph]
[10] Halzen F and O'Murchadha A 2008 arXiv:0802.0887 [astro-ph]
[11] Gupta N 2008 arXiv:0804.3017 [astro-ph]
[12] Israel F P 1998 *Astron. Astrophys. Rev.* **8** 237 (arXiv:astro-ph/9811051)
[13] Steinle H 2006 *Chin. J. Astron. Astrophys. Suppl.* **6** 106
[14] Rejkuba M 2004 *Astron. Astrophys.* **413** 903 (arXiv:astro-ph/0310639)
[15] Shakura N I and Syunyaev R A 1973 *Astron. Astrophys.* **24** 337
Chakrabarti S K 1996 *Phys. Rep.* **266** 229
[16] Silge J D, Gebhardt K, Bergmann M and Richstone D 2005 *Astron. J.* **130** 406 (arXiv:astro-ph/0501446)
Marconi A *et al* 2006 *Astron. Astrophys.* **448** 921 (arXiv:astro-ph/0507435)
Neumayer N *et al* 2007 arXiv:0709.1877 [astro-ph]
[17] Evans D A *et al* 2004 *Astrophys. J.* **612** 786 (arXiv:astro-ph/0405539)
[18] Evans D A 2008 private communication
[19] Hardcastle M J, Evans D A and Croston J H 2007 *Mon. Not. R. Astron. Soc.* **376** 1849 (arXiv:astro-ph/0701857)
[20] Markowitz A *et al* 2007 *Astrophys. J.* **665** 209 (arXiv:0704.3743 [astro-ph])
[21] Malkan M A and Sargent W L W 1982 *Astrophys. J.* **254** 22
[22] Mouri H 1994 *Astrophys. J.* **427** 777
[23] Laor A and Netzer H 1989 *Mon. Not. R. Astron. Soc.* **238** 897
[24] Atoyan A and Dermer C D 2001 *Phys. Rev. Lett.* **87** 221102 (arXiv:astro-ph/0108053)
[25] Steinle H *et al* 1998 *Astron. Astrophys.* **330** 97
[26] Kachelrieß M, Parizot E and Semikoz D V 2008 *Pis. Zh. Eksp. Teor. Fiz.* **88** 663–7
[27] Kraft R P *et al* 2003 *Astrophys. J.* **592** 129 (arXiv:astro-ph/0304363)
[28] Worrall D M *et al* 2007 arXiv:0712.3579 [astro-ph]
[29] Graham J A 1979 *Astrophys. J.* **232** 60
Jones D L *et al* 1996 *Astrophys. J.* **466** L63 (arXiv:astro-ph/9606023)
[30] Kazanas D and Ellison D C 1986 *Astrophys. J.* **304** 178
[31] Berezinsky V 1994 *Phil. Trans. R. Soc.* A **346** 95
[32] Blandford R D 1976 *Mon. Not. R. Astron. Soc.* **176** 465
[33] Lovelace R V E 1976 *Nature* **262** 649
[34] Blandford R D and Znajek R L 1977 *Mon. Not. R. Astron. Soc.* **179** 433
[35] MacDonald D and Thorne K S 1982 *Mon. Not. R. Astron. Soc.* **198** 345
[36] Rachen J P and Biermann P L 1993 *Astron. Astrophys.* **272** 161 (arXiv:astro-ph/9301010)
Rachen J P, Stanev T and Biermann P L 1993 *Astron. Astrophys.* **273** 377 (arXiv:astro-ph/9302005)
[37] Romero G E, Combi J A, Anchordoqui L A and Perez Bergliaffa S E 1996 *Astropart. Phys.* **5** 279 (arXiv:gr-qc/9511031)
[38] Casse F, Lemoine M and Pelletier G 2002 *Phys. Rev.* D **65** 023002 (arXiv:astro-ph/0109223)
[39] Berezinsky V, Gazizov A Z and Grigorieva S I 2002 arXiv:hep-ph/0204357
Berezinsky V, Gazizov A Z and Grigorieva S I 2004 *Nucl. Phys.* B **136** 147 (arXiv:astro-ph/0410650)
Berezinsky V, Gazizov A Z and Grigorieva S I 2005 *Phys. Lett.* B **612** 147 (arXiv:astro-ph/0502550)

[40] Kachelrieß M and Semikoz D V 2006 *Phys. Lett.* B **634** 143 (arXiv:astro-ph/0510188)
[41] Kachelrieß M and Tomàs R 2006 *Phys. Rev.* D **74** 063009 (arXiv:astro-ph/0606406)
Kachelrieß M, Ostapchenko S and Tomàs R 2008 *Phys. Rev.* D **77** 023007 (arXiv:0708.3047 [astro-ph])
[42] Sjostrand T 1995 arXiv:hep-ph/9508391
Fletcher R S, Gaisser T K, Lipari P and Stanev T 1994 *Phys. Rev.* D **50** 5710
Mücke A *et al* 2000 *Comput. Phys. Commun.* **124** 290 (arXiv:astro-ph/9903478)
Ostapchenko S 2006 *Nucl. Phys.* B **151** 143 (arXiv:hep-ph/0412332)
Ostapchenko S 2006 *Phys. Rev.* D **74** 014026 (arXiv:hep-ph/0505259)
[43] Aharonian F A, Coppi P S and Volk H J 1994 *Astrophys. J.* **423** L5 (arXiv:astro-ph/9312045)
Neronov A and Semikoz D V 2007 *JETP Lett.* **85** 473 (arXiv:astro-ph/0604607)
[44] Aharonian F *et al* [HESS Collaboration] 2005 *Astron. Astrophys.* **441** 465 (arXiv:astro-ph/0507207)
[45] Morselli A 2003 *Chin. J. Astron. Astrophys. Suppl.* **3** 523 Available at http://people.roma2.infn.it/~glast/A102Morselli_Vulcano03.pdf
[46] Nadolsky P M *et al* arXiv:0802.0007 [hep-ph]
[47] Gandhi R, Quigg C, Reno M H and Sarcevic I 1996 *Astropart. Phys.* **5** 81 (arXiv:hep-ph/9512364)
[48] Neronov A Y and Semikoz D V 2002 *Phys. Rev.* D **66** 123003 (arXiv:hep-ph/0208248)
[49] Fargion D 2008 arXiv:0801.0227 [astro-ph]
Fargion D 2008 arXiv:0804.1088 [astro-ph]
Rachen J P 2008 arXiv:0808.0349 [astro-ph]